

Robust estimation of MRI myocardial perfusion parameters

Santiago Aja-Fernández, Lucilio Cordero-Grande, Gonzalo Vegas-Sanchez-Ferrero,
Rodrigo de Luis-García, Carlos Alberola-López

Abstract—Myocardial perfusion imaging by first-pass contrast-enhanced magnetic resonance allows to assess the viability of a tissue by the study of the contrast agent transit through the cardiac chambers and myocardium. Since visual inspection is difficult and may left aside critical temporal information, the need of automatic quantitative analysis arises. We propose two robust estimators of the parameters that quantify the perfusion according to a prior pharmacokinetic model. The estimators are based on the concentration of the contrast agent inside the tissue and the blood.

Index Terms—Magnetic resonance, robust estimation, myocardial perfusion imaging.

I. INTRODUCTION

Myocardial perfusion imaging by first-pass contrast-enhanced magnetic resonance (MR) [1], [2] is obtained after injection of a bolus of a contrast agent such as Gadolinium (Gd-DTPA), which induces variations in the measured signal (specifically the longitudinal relaxation time T_1) across the different tissues. The aim of this technique is to measure the perfusion characteristics of each of the tissues of the myocardium from the received temporal signal. This analysis can be carried out in a qualitative way by visual inspection [3], semi-quantitative (using descriptive parameters) or in a quantitative way [4] by estimating some parameters linked to a prior pharmacokinetic model.

The analysis of the images by visual inspection is a difficult task mainly due to the dynamic nature of the perfusion. If the temporal information of the sequence is neglected, important knowledge about the characterization of the diffusion inside the tissues may be left aside [2]. Alternatively, quantitative analysis has the advantage of taking into account the different sources of information, spatial and temporal. On the other hand, it requires the estimation of some perfusion parameters. This estimation is not a simple task when dealing with MR data, and it becomes more complex in cardiac imaging as opposed to static organs.

An automatic perfusion assessment process from MR data involves three steps: (a) Image processing: heart, patient and breathing motion must be corrected, and the regions of interest (in this case the myocardium) have to be identified and segmented; (b) Extraction of the concentration signals from the MR signals. The concentration of the contrast agent is inversely proportional to the variation of time T_1

The authors are with the LPI, ETSI Telecomunicación, Universidad de Valladolid, Spain. This work was partially supported by CDTI (cvREMODO, ref. CEN-20091044), Junta de Castilla y León (VA0339A10-2, SAN103/VA40/11, GRS 555/A/10) and MICIN (TEC2010-17982). Authors acknowledge Quirón (Valencia) and J. Sanchez Gonzalez for the collaboration in cardiac sequence acquisition. Contact: sanaja@tel.uva.es.

inside the tissues. Thus, the concentration signals are to be estimated from the T_1 mapped from the intensity image using the specific acquisition parameters; (c) Deconvolution of the tissue transit signal or estimation of the parameters of the prior pharmacokinetic model. First of all, it is necessary to estimate the arterial input function (AIF), which gives a measure of the concentration of the contrast agent in the blood. The AIF is considered as the input signal to the system.

In the present work we theoretically study the myocardial perfusion pharmacokinetic model. We propose two robust estimators of the parameters that quantify the perfusion according to that model. The validation of the proposed estimators is mainly done using synthetically generated data, in order to avoid external issues that can bias or alter the estimation (like the segmentation or the temporal alignment of MR sequences).

II. ROBUST ESTIMATION OF PERFUSION PARAMETERS

A. Pharmacokinetic modeling of myocardial perfusion

Many models and methods have been proposed in literature in order to carry out an automatic analysis of the perfusion [4]. However, they have not been totally adapted to the specific needs of myocardial perfusion, since it presents some constraints due to scanning time, heartbeats and breathing movement that make the final images and models differ from other common MR perfusion modalities, such as brain or abdominal.

In the following sections we will work with two signals: the concentration of the contrast agent in tissue, $c(t)$, and in blood, $c_a(t)$. We assume that (1) these concentrations are feasible to be estimated from the T_1 maps from the scanner; (2) we are capable to properly measure the AIF that gives the concentration of contrast agent in blood.

For the perfusion modeling, we also assume a compartmental model of the tissue, specifically the two-compartment modeling (blood plasma and extravascular/extracellular space) proposed in [4]. Inside each compartment (or kind of tissue) the contrast distribution is assumed to be homogeneous. This implies a diffusion of the agent much faster inside each compartment than its transfer among compartments.

In the myocardium, where only one blood apportion exists, the relation between the arterial and tissue concentration is given by the following equation:

$$\frac{dc(t)}{dt} = K_T c_a(t) - K_e c(t) \quad (1)$$

where K_T represents the kinetic rate constant of transfer of the contrast agent flow from the vasculature into the extravascular/extracellular space inside the myocardium and K_e is the kinetic rate into the myocardial vasculature. Both of them are related by parameter v_e , which represents the fractional volume of extravascular/extracellular space (or flow extraction product), which is always bounded: $0 < v_e < 1$.

From eq. (1), the relation between $c(t)$ and $c_a(t)$ can be written as a convolution:

$$c(t) = c_a(t) * r(t). \quad (2)$$

where signal $r(t)$ is the impulse response of the tissue, that can be easily derived from eq. (1):

$$r(t) = K_T \cdot e^{-K_e t} u(t) \quad (3)$$

with $u(t)$ the Heaviside step function.

The relation in eq. (2) can be written in the Fourier domain as:

$$C(\omega) = C_a(\omega)R(\omega) = C_a(\omega) \frac{K_T}{j\omega + K_e} \quad (4)$$

All this modeling implies initial rest for signals $c_a(t)$ and $c(t)$.

B. Estimation of Fractional Volume v_e

Perfusion parameters have been traditionally estimated from eq. (4) via some deconvolution method such as:

$$R(\omega) = \frac{C(\omega)}{C_a(\omega)} \xrightarrow{\mathcal{F}^{-1}} r(t).$$

Despite of being theoretically correct in its continuous formulation, this methodology may present serious drawbacks due to the discrete nature of the measures. The inevitable aliasing when sampling the temporal signal together with a method based on the inverse Fourier transform may bias the estimation or generate serious instabilities. Some authors try to *compensate* the aliasing using interpolation methods like splines [5]. However, note that the estimation of signal $r(t)$ is not necessary for perfusion quantification: only parameters K_T and K_e are relevant. Many studies, in fact, only need of fractional volume $v_e = K_T/K_e$ for perfusion assessment [4].

In this section we will first propose a method to estimate the fractional volume v_e . From eq. (4) we can calculate the Fourier Transform at the origin:

$$C(0) = C_a(0) \frac{K_T}{0 + K_e} = C_a(0) v_e. \quad (5)$$

From here we can write v_e as

$$v_e = \frac{K_T}{K_e} = \left[\frac{C(\omega)}{C_a(\omega)} \right]_{\omega=0} = \frac{\int_0^\infty c(t) dt}{\int_0^\infty c_a(t) dt} \quad (6)$$

Thus, the volume v_e can be calculated as a ratio between the area below curves of concentration in tissue and in blood.

Since the measured data are discrete, the integrals are to be approximated by sums.

$$v_e = \frac{K_T}{K_e} = \frac{\sum_{n=1}^N c[n] \Delta t}{\sum_{n=1}^N c_a[n] \Delta t} = \frac{\sum_{n=1}^N c[n]}{\sum_{n=1}^N c_a[n]} \quad (7)$$

Note that, since the area below the AIF is the same for all the pixels in the image, the denominator in eq. (7) can be seen as a constant for all tissues. Volume v_e will therefore be proportional to the area of concentration in each tissue. An error in the measure of the AIF will proportionally affect all the tissues in the same way and the ratio of v_e between tissues will remain constant:

$$\frac{v_{e1}}{v_{e2}} = \frac{\int_0^\infty c_1(t) dt}{\int_0^\infty c_a(t) dt} \cdot \frac{\int_0^\infty c_a(t) dt}{\int_0^\infty c_2(t) dt} = \frac{\int_0^\infty c_1(t) dt}{\int_0^\infty c_2(t) dt}$$

On the other hand, an estimation based on integration (as opposed to those methods based on deconvolution) will be more robust to noise and measure errors.

C. Estimation of parameter K_e

To carry out a robust estimation of parameter K_e , we integrate the convolution in eq. (2):

$$\int_{-\infty}^t c(\tau) d\tau = \int_{-\infty}^t c_a(\tau) * r(\tau) d\tau = c_a(t) * \int_{-\infty}^t r(\tau) d\tau.$$

Since we assume initial rest for all the signals, the lower limits can be changed to zero:

$$\begin{aligned} \int_{-\infty}^t r(\tau) d\tau &= \int_0^t K_T e^{-K_e \tau} u(\tau) d\tau \\ &= \frac{K_T}{K_e} u(t) - \frac{K_T}{K_e} e^{-K_e t} u(t) \\ &= v_e \cdot u(t) - \frac{1}{K_e} r(t) \end{aligned}$$

and then

$$\begin{aligned} \int_{-\infty}^t c(\tau) d\tau &= c_a(t) * \left(v_e \cdot u(t) - \frac{1}{K_e} r(t) \right) \\ &= c_a(t) * (v_e \cdot u(t)) - \frac{1}{K_e} \underbrace{c_a(t) * r(t)}_{c(t)} \\ &= v_e \left(\int_0^t c_a(\tau) d\tau \right) \cdot u(t) - \frac{1}{K_e} c(t) \end{aligned}$$

Even though the expression above lets us directly estimate K_e , for the sake of robustness we have resorted to estimate it as $\widehat{K_e} = \arg \min \int_0^\infty |f(t; K_e)|^2 dt$ with

$$f(t; K_e) = \int_{-\infty}^t c(\tau) d\tau - v_e \left[\int_0^t c_a(\tau) d\tau \right] + \frac{1}{K_e} c(t)$$

After some algebra:

$$\widehat{K_e} = \frac{\int_0^\infty c^2(t) dt}{\int_0^\infty c(t) \left[v_e \int_0^t c_a(\tau) d\tau - \int_0^t c(\tau) d\tau \right] dt} \quad (8)$$

Note that once K_e and v_e are estimated, the calculation of K_T is straightforward.

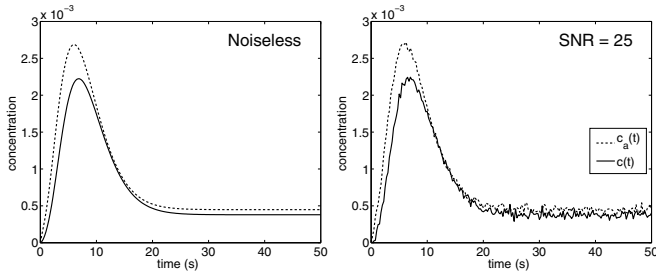


Fig. 1. Synthetic concentration agent curves generated from the continuous model. Sampling rate $\Delta t = 0.25$ s.

	Proposed				LS	
	$\Delta t = 0.25$		$\Delta t = 1$		$\Delta t = 0.25$	
	v_e	K_e	v_e	K_e	v_e	K_e
Real	0.84	1.30	0.84	1.30	0.84	1.30
Est. (Noiseless)	0.84	1.30	0.84	1.34	0.73	1.14
Est. (SNR=25)	0.84	1.42	0.84	1.53	0.71	1.01
Est. (SNR=10)	0.85	1.11	0.83	1.38	0.74	1.14

TABLE I
ESTIMATION OF PERFUSION PARAMETERS FOR THE SYNTHETIC EXPERIMENT.

III. EXPERIMENTS AND RESULTS

To test the performance of the proposed estimators, we first carry out a synthetic experiment. In order to simulate the concentration of the contrast agent, a continuous theoretical model is considered, as proposed in [6]. Since both $c_a(t)$ and $c(t)$ are continuous-time processes in nature, the effect of the aliasing over the estimation can be controlled. For the sake of simplicity, the AIF is modeled as a Gamma distribution (for the main lobe) and a decreasing exponential (for the tail):

$$c_a(t) = M_1 \cdot \frac{t^{a-1} e^{-t/b}}{\Gamma(a)b^2} u(t) + M_2 \cdot (1 - e^{-t/d}) u(t) \quad (9)$$

with a, b, d , the shape parameters and M_1 and M_2 scaling constants. In our experiment we will work with $M_1 = 0.02$, $a = 4$, $b = 2$, $c = 1$ and $M_2 = \max\{c_a(t)\}/5$. In order to obtain $c(t)$, the analytical convolution with $r(t)$ is calculated:

$$c(t) = M_1 \cdot r(t) \cdot \frac{\gamma_i(a, t(\frac{1}{b} - K_e))}{(1 - K_e \cdot b)^a} + M_2 \cdot K_t \cdot \left(\frac{1 - e^{-K_e t}}{K_e} - \frac{e^{-t} - e^{-K_e t}}{K_e - 1} \right) \quad (10)$$

with $\gamma_i(\cdot)$ the incomplete Gamma function. Discrete sequences are obtained by sampling both concentration signals with $K_e = 1.3$, $K_T = 1.1$, sampling rate $\Delta t = 0.25$ and $t = 50$ seconds. The signals are depicted in Fig. 1 (left). Additive Gaussian noise with zero mean is added to the signal to obtain a SNR=25, see Fig. 1 (right).

Parameters v_e and K_e are estimated using the proposed methods. Results are shown in Table I. For comparison, the parameters are also estimated using a standard Least Squares (LS) fitting over the model in eq. (2) To take into account

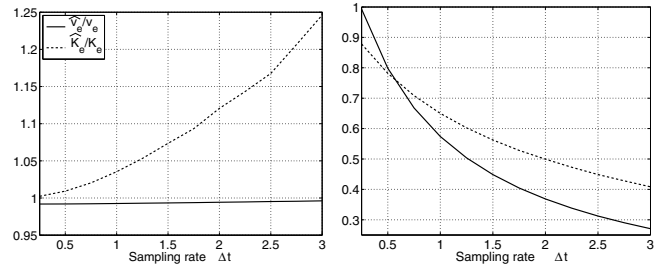


Fig. 2. Evolution of the estimators with the sampling rate. Proposed method (left) and Least Squares fitting (right).

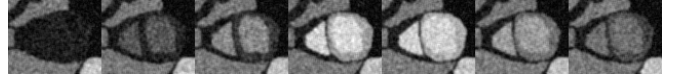


Fig. 3. One slice of the MR myocardial perfusion phantom.

the robustness of the estimation to aliasing, the experiment is repeated for $\Delta t = 1$. In both cases, the estimation of parameter v_e , is robust to noise and aliasing, due to the integral formulation. The second estimator is more sensitive to the artifacts, due to the more complex formulation and the difference of two related functions in the denominator in eq. (8). Nevertheless, in both cases the estimation is more accurate than the one carried out by LS. This methods fails due to the aliasing existing in the discrete model when assuming eq. (8).

Finally, in Fig. 2 both estimators are depicted for a wide range of sampling rates (from 0.25s to 3s). As a quality measure we have used the ratio between the estimated and the real values: $[\hat{v}_e/v_e, \hat{K}_e/K_e]$. The closer to 1 the better the estimation. Note that \hat{v}_e is a very good estimator even for large sampling rates. On the other hand, \hat{K}_e worsens as Δt grows, as expected. In any case, both estimators are much more robust than the standard LS.

For a more realistic validation, we test now the estimators with the 2D cardiac perfusion phantom proposed in [6]. A single coil sequence is simulated with correlated Rician noise ($\sigma_n = 15$), partial volume effect (PVE), $r_1 = 4.5$, TR=2.7290 ms, $\Delta t = 0.75$ s, 50 samples, $K_T = 0.4$, $K_e = 0.9$ for the tissue and $K_T = 0.5$, $K_e = 0.6$ for the scar. An illustration of the simulated sequence is shown in Fig. 3.

The intensity curves are extracted for each pixel in blood and tissue. In order to smooth the curves, a 4-class clustering is carried out for the myocardium curves. Concentration curves $c_t(t)$ and $c_a(t)$ are then estimated from the intensity curves [4], [5]. Parameters v_e and K_e are estimated for each of the pixels in the myocardium wall and results are shown in Fig. 4. Note that, although the scar is barely visible by visual inspection in Fig. 3, it is now visible in the estimated values. Note also that, due to the PVE, some *extra class* has appeared in the outer border of the myocardium. Since it is clearly an artifact, it can be neglected in further analysis. On the other hand, the estimated values match the values used for simulation. Only the K_e value in the scar is slightly biased.

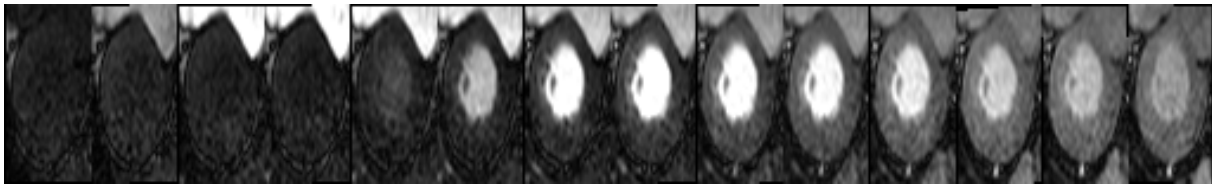


Fig. 5. One slice of the MR myocardial perfusion sequence. ($\Delta t = 0.5$, 10mm slices, 76 temporal samples, acquired in a Philips Intera 1.5T scanner using fast field echo MAG).

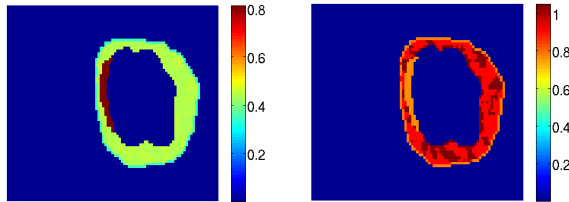


Fig. 4. Estimation of perfusion parameters for the phantom: Fractional volume estimation, \hat{v}_e (left) and parameter K_e (right) using a 4-class clustering.

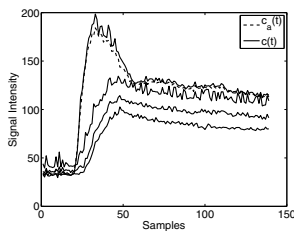


Fig. 6. Intensity curves for the myocardial perfusion sequence after a 4-class clustering.

Finally, an experiment with real data is done. An MR myocardial perfusion sequence is considered, with $\Delta t = 0.5$, 3 slices of 10mm and 76 temporal samples, acquired in a Philips Intera 1.5T scanner using fast field echo MAG. A presaturation spatial pulse has been applied, and a flip angle $\alpha = 50^\circ$, see Fig. 5.

First of all, temporal data have been processed to correct the misalignment due to the breathing movement, following the method in [7]. Secondly, the myocardium and the left ventricle are segmented using a small modification of the method proposed in [8]. The intensity curves for each pixel in blood and tissue are traced and a 4-class clustering is carried out again. Results are shown in Fig. 6.

Considering these 4 classes, volume v_e is estimated for each of the pixels in the myocardium wall. Results are shown in Fig. 7 for 3 slices. There is an area in the upper side of the second slice where the estimated v_e shows a value larger than the rest of the heart, being a possible indicator of a scar area. In addition, note that values of the *green* and *yellow* areas are very close, and they probably belong to the same kind of tissue with slight variations.

IV. CONCLUSIONS

A new methodology to estimate the parameters of myocardial perfusion images is proposed. The method has

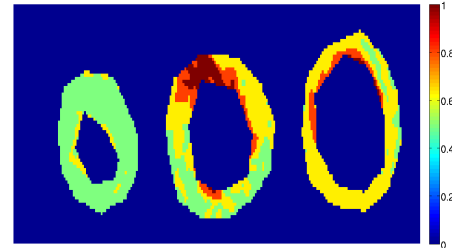


Fig. 7. Fractional volume estimation, \hat{v}_e , for the 3 cardiac slices in the myocardial perfusion sequence after a 4-class clustering

the following advantages: (1) since it is based on integral formulation it is more robust than those methods based on deconvolution; (2) It is robust against a wrong estimation of the AIF: the volume v_e , eq (7) is proportional to the area below the $c(t)$ curve. An error in the estimation of $c_a(t)$ will equally bias the estimation of all the tissues. The method has shown to be robust in different experiments based on theoretical models, and it also shows promising results in real data.

REFERENCES

- [1] M. Jerosch-Herold, Ravi Teja Seethamraju, Cory M. Swingen, Norbert M. Wilke, and Arthur E. Stillman, "Analysis of myocardial perfusion MRI," *J. Magn. Reson.*, vol. 19, no. 6, pp. 758–770, 2004.
- [2] Bernhard L Gerber and *et al.*, "Myocardial first-pass perfusion cardiovascular magnetic resonance: history, theory, and current state of the art," *J. Card. Mag. Res.*, vol. 10, no. 18, 2008.
- [3] B. Preim and *et al.*, "Survey of the visual exploration and analysis of perfusion data," *IEEE Trans. Visualization and Comp. Graphics*, vol. 15, no. 2, pp. 205–220, 2009.
- [4] P. S. Tofts and *et al.*, "Estimating kinetic parameters from dynamic contrast-enhanced T1-weighted MRI of a diffusable tracer: Standardized quantities and symbols," *J. Magn. Reson.*, vol. 10, no. 3, pp. 223–232, 1999.
- [5] V.J. Schmid, B. Whitcher, A.R. Padhani, and Guang-Zhong Yang, "Quantitative analysis of dynamic contrast-enhanced MR images based on Bayesian P-splines," *IEEE Trans. Med. Imaging*, vol. 28, no. 6, pp. 789–798, 2009.
- [6] S. Aja-Fernández, L. Cordero-Grande, and C. Alberola-López, "A mri phantom for cardiac perfusion simulation," in *Biomedical Imaging (ISBI), 2012 9th IEEE International Symposium on*, may 2012, pp. 638–641.
- [7] L. Cordero-Grande, S. Merino-Caviedes, R. de Luis-García, S. Aja-Fernández, M. Martín-Fernández, and C. Alberola-López, "Groupwise myocardial alignment in magnetic resonance perfusion sequences," in *Proc of the XXIX CASEIB*, Cáceres, Spain, 2011, pp. 437–440.
- [8] Cordero-Grande L, Vegas-Sánchez-Ferrero G, Casaseca de-la Higuera P, San-Román-Calvar JA, Revilla-Orodea A, and Alberola-López C. Martín-Fernandez M, "Unsupervised 4D cardiac image segmentation with a Markov random field based deformable model," *Medical Image Analysis*, vol. 15, pp. 283–301, 2011.